Journal Name

COMMUNICATION

Fluorescence Lifetime Imaging of Intracellular Magnesium Content in Live Cells

Received 00th January 20xx,
Accepted 00th January 20xx

DOI: 10.1039/x0xx00000x

www.rsc.org/

Azzurra Sargenti, [a§] Alessia Candeo, [b§] Giovanna Farruggia, [a,c] Cosimo D'Andrea, [b] Concettina Cappadone, [a] Emil Malucelli, [a] Gianluca Valentini, [b] Paola Taroni, [b] Stefano Iotti [a,c*]

The first detailed analysis of FLIM applications for Mg cell imaging is presented. We employed the Mg-sensitive fluorescent dye named DCHQ5, a derivative of diaza-18-crown-6 ethers appended with two 8-hydroxyquinoline groups, to perform fluorescence lifetime imaging in control and Mg deprived SaOS-2 live cells, which contain different concentration of magnesium. We found that the lifetime maps are almost uniform all over the cells and, most relevant, we showed that the ratio of the amplitude terms is related to the magnesium intracellular concentration.

Fluorescence lifetime imaging (FLIM) represents an established method for live-cell imaging and can provide novel information from intact cellular environments.[1,2] This technique allows one to generate image contrast based on the decay time of endogenous fluorophores or sensing dyes at each point in a two-dimensional image.[3,4] Most fluorescent dyes undergo a change in the fluorescence lifetime upon binding their specific ion. Therefore, FLIM may be exploited for imaging intracellular ions without the need for wavelength-ratiometric probes, bearing the same advantages, such as no bias from fluorophore concentration and/or excitation intensity, light path length and photobleaching.[5] Moreover, changes in the physicochemical intracellular microenvironment of density, pH and lipophilicity may have substantial effects on the fluorescence lifetime of a fluorophore, and FLIM may in principle exploit the natural heterogeneity of cells and tissues, turning this information into image contrast.

[a] Department of Pharmacy and Biotechnology, University of Bologna, Bologna, Italy.
[b] Department of Physics, Politecnico di Milano, Piazza Leonardo da Vinci 32, 20113, Milano, Italy.
[c] National Institute of Biostructures and Biosistems (NIBB), Rome, Italy.
§These authors equally contributed to these work

* Corresponding Author

Electronic Supplementary Information (ESI) available: [details of any supplementary information available should be included here]. See DOI: 10.1039/x0xx00000x

FLIM disentangles the contributions to fluorescence intensity that come from fluorophore concentration and time behaviour of the fluorescence decay. Thus, it can also be exploited to gain a deeper insight into results obtained through conventional steady state fluorescence imaging (e.g., confocal microscopy), which is actually fluorescence intensity imaging.

Commercial magnesium (Mg) dyes have been characterized for FLIM applications,[6] although at present no further experimental studies have been reported in literature. The aforementioned features of FLIM could be employed to acquire information on magnesium content and distribution in subcellular compartments with different composition. The development of novel sensors exhibiting discriminating lifetimes[7–9] marks a step further in this direction.

We have designed and characterized a panel of some derivatives of diaza-18-crown-6 ethers appended with two 8-hydroxyquinoline groups (DCHQs) that carry task-specific substituents in position 2, 4 or 5 of the quinoline ring system. This results in sensing dyes that show interesting applications to measure the cell magnesium content and distribution. [10,11] The photophysical properties of this class of compounds are determined by the presence of the derivatives of the well-known 8-hydroxyquinoline dye. Among these, the probe named DCHQ5, composed of an N,N'-bis-((8-hydroxy-7-quinolinyl)methyl)-1,10-diaza-18-crown-6 ether bearing a

phenyl group as a substituent in position 5 of each hydroxyquinoline arm (Fig. 1A), showed prominent features

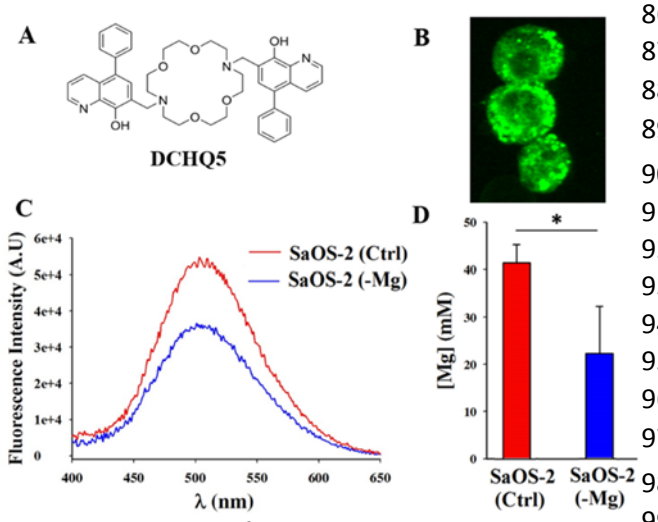

Fig. 1 Characteristics of DCHQ5:
A) Chemical structure of DCHQ5.
B) Confocal microscopy image (λexc = 488 nm) of SaOS-2 human osteosarcoma cells stained with DCHQ5 10 μM.
C) DCHQ5 (15 μM) fluorescence spectra (λexc = 360 nm) of sonicated samples of control (Ctrl, red line) and Mg-deprived (-Mg, blue line) SaOS-2 cells. Results from a typical experiment.
D) Total intracellular Mg concentrations quantified by fluorimetric DCHQ5 assay [12,13] in sonicated samples of control (Ctrl, red bar) and Mg-deprived (-Mg, blue bar) SaOS-2 cells. The concentrations assessed were 41.4 ± 3.9 mM and 22.3 ± 9.9 mM respectively. Data are reported as mean ± SD. Statistical significance was determined using Student's t test (*$p < 0.05$).

In fact, the fluorescent dye DCHQ5 owns the unique analytical capability to quantify the total intracellular magnesium content by fluorimetric assay and shows enhanced characteristics as compared with the other members of the panel.[12] It displays high fluorescence intensity upon cation binding (Fig. 1C) and intense intracellular staining (Fig. 1B), great intracellular retention and a notable fluorescence signal stability.[10] Furthermore, it provides the advantage of effective excitation both in the UV and visible (488 nm) wavelengths ranges,[11] opening the possibility to exploit the dye for FLIM measurements.

Indeed, it is known that in biological samples the autofluorescence might present serious competition with exogenous dyes in lifetime imaging, and it is typically stronger at shorter wavelengths. At this extent, green-fluorescent dyes commercially available, with excitation ideally suited to the 488 nm laser line, were used to differentiate between the extrinsic label and the autofluorescence.[14] The fluorescence decay of several members of the DCHQ family were examined in different cell lines by single-photon counting spectrofluorimetry. The decay can be conveniently fitted only if two different excited-state lifetimes are considered. The two observed lifetimes are similar in the different cell lines for all the dyes tested, with a short decay time τ1 (few ns) and a much longer decay time τ2 (>10 ns).[7]

It is unlikely that the two lifetimes reflect the bound and unbound state of the dye due to the DCHQ5 physical chemical properties[11]. In fact, we reported that i) the fluorescence of the dye bound to Mg is up to 21 times higher than the fluorescence intensity of the unbound DCHQ5; and ii) the proportion of the unbound dye is by several orders of magnitude lower of the bound dye due to the very low Kd of DCHQ5 (83 μM)[11].

The most straightforward interpretation of the existence of two families of excited-states characterized by different lifetimes is that the probe molecules are surrounded by two different environments, a more polar one that is likely the cytosol, resulting in τ1, and a less polar one when the probe is localized, for example in membranes, leading to τ2. Indeed, there is experimental evidence that hydrophobic derivatives of hydroxyquinoline preferentially distribute into lipophilic moieties.[15] Hence, the hydrophobic nature of DCHQ dyes and the aforementioned lifetime measurements could led to hypothesize that the fluorescence enhancement obtained in intact cells is generated by the entrapment of the probe in membrane compartments.[16] However, this characteristic would represent a serious drawback, preventing the use of the fluorescent dye for magnesium quantitative assessment in live cells by confocal imaging. Different lifetimes corresponding to different intracellular compartments may in principle hamper the assessment of the intracellular content of Mg by steady state imaging techniques. In fact, the fluorescence quantum yield is proportional to the fluorescence lifetime[16] and the enhancement of the fluorescence signal in certain regions of the cell could wrongly be ascribed to a higher Mg concentration. Therefore, the need to explore the intracellular spatial distribution of the fluorescence decay of the dye becomes of paramount importance. This information will provide the experimental evidence about the possibility to expand the application of the DCHQ5 dye to quantitative imaging techniques.

In addition to inspect whether the spatial distribution of lifetimes is influenced by the dye compartmentalization, we also wanted to inspect how in the same cellular environment (i.e. same cell type) a different Mg content affects FLIM maps.

To this aim, we exploited two sister cell lines SaOS-2: control and Mg-deprived, purposely prepared to contain different amount of total intracellular Mg (see supplementary information). The total intracellular Mg concentrations of these two cell lines was quantified by fluorimetric DCHQ5 assay resulting to be: 41.4 ± 3.9 mM in control SaOS-2 and 22.3 ± 9.9 mM in Mg-deprived SaOS-2 as reported in (Fig. 1D). We employed the DCHQ5 dye to perform fluorescence lifetime imaging in samples of the same control and Mg-deprived SaOS-2 live cells to explore: i) the capability of this dye to provide FLIM maps under visible light excitation; ii) the implications for magnesium assessment in cells that derive from an uneven distribution of excited-states with different lifetimes; and iii) the possible FLIM applications for quantitative biological imaging of magnesium. As a typical example of the results obtained, Fig. 2B reports the decay curves measured from two different areas (the AOIs indicated in the steady state fluorescence image in Fig. 2A) of a SaOS-2 cell. The best model to account for the fluorescence of all the cells considered in the present experiment proved to be a bi-exponential function with an offset, which was included in the model to account for and allow the removal of any unspecific long living emission, mainly due to the optical elements (especially the microscope objective). The bi-exponential fitting, consistently with previous experiments, identified a short decay time $\tau 1$ with higher amplitude A1 and ten-fold longer decay time $\tau 2$ with corresponding lower amplitude A2 (Fig. 2C). Comparable lifetime values were measured from both areas, despite the different intensity. Actually, the strong difference in the steady state fluorescence signal detected from the two areas can be attributed only to the amplitudes, which both reduce by a factor of two in the AOI 2, characterized by weaker fluorescence, thus leaving the ratio of the amplitude terms roughly unchanged.

Fig. 3 shows the lifetime and amplitude maps for the same SaOS-2 cell as in Fig. 2. The maps present the typical “salt and pepper” noise (Poisson noise) ascribable to the limited number of photons per pixel that mainly affects the images acquired at long delays after the excitation pulses.

Notwithstanding the noise, the lifetime maps (Fig. 3C and D) show neither spatial features, nor any correlation with the steady state fluorescence intensity (Fig. 2A). At variance, the amplitude maps match the pattern of the steady state fluorescence image. This confirms that the spatial variation of the fluorescence intensity stems from the amplitude variation, which, according to a simple model, measures the spatial concentration of the probe. Consistent results were obtained for all control SaOS-2 cells. To test the dependence of the fluorescence lifetimes maps and their amplitudes on the intracellular concentration of magnesium, FLIM was performed also on Mg-deprived SaOS-2 (-Mg) cells.

The experiment confirmed the insensitivity of the lifetime values to the magnesium concentration, which instead affects significantly the amplitude ratio (A1/A2) of the short living vs. long living fluorescent components. Fig. 4 displays the boxplots of the lifetime ratio and the amplitude ratio for both cell types (control (Ctrl) and Mg-deprived (-Mg) SaOS-2), showing that comparable lifetime ratio is measured

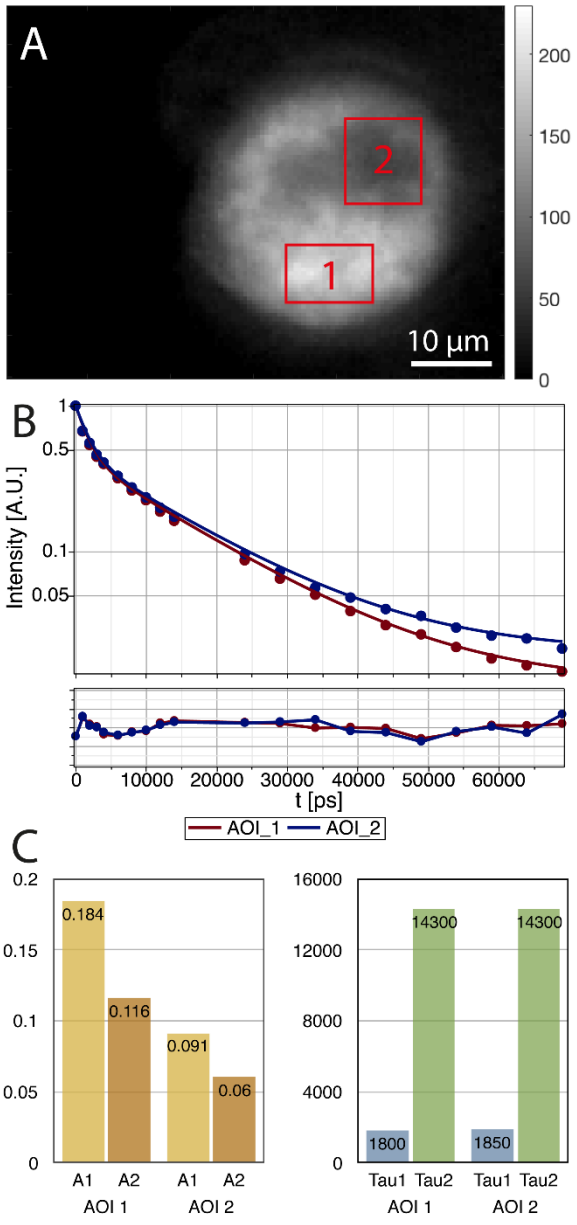

Fig. 2 A) Steady state fluorescence image of a typical SaOS-2 cell; B) Examples of bi-exponential fit with residuals on the fluorescence emission decay integrated over the pixels of AOI 1, (high intensity) and AOI 2 (low intensity); C) Histograms of the amplitudes (a.u.) and lifetimes (ns) in AOIs 1 and 2.

independent of the magnesium concentration, while the amplitude ratio is significantly higher for control SaOS-2 cells than for deprived ones (Mann-Whitney test, $p < 0.0001$). This result indicates that the amplitudes of the DCHQ5 fluorescence components are related to the average Mg intracellular content. Further, by the amplitude ratio (A1/A2) it is possible to distinguish between cells having a difference of about 20 mM in their total intracellular Mg concentration, as the case of the sister cell lines employed in this study (Fig. 1D). However, the fluctuation of Mg concentration within a single cell is much smaller,[17] making more challenging the task of mapping local Mg intracellular compartmentalization. In fact, in all the single cells analyzed we did not find a statistical relevant difference in the amplitude ratio (A1/A2) between the AOIs corresponding to different steady state fluorescence intensities, although the data reported in Fig. 3 might suggest a trend in the expected direction.

AOI	A1 [A.U.]	A2 [A.U.]	Tau1 [ps]	Tau2 [ps]	A1%	A2%	A1/A2
1	0.18	0.12	1800	14300	61	39	1.59
2	0.09	0.06	1850	14300	60	40	1.52

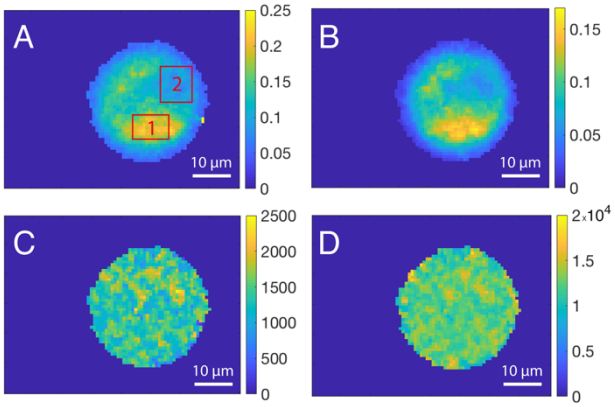

Fig. 3 Amplitude (a.u., A and B) and lifetime (ns, C and D) maps of the short (A, C) and long (B, D) living fluorescent components measured in the SaOS-2 cell shown in Fig. 2.

The experiment confirmed the insensitivity of the lifetime values to the magnesium concentration, which instead affects significantly the amplitude ratio (A1/A2) of the short living vs. long living fluorescent components. Fig. 4 displays the boxplots of the lifetime ratio and the amplitude ratio for both cell types (control (Ctrl) and Mg-deprived (-Mg) SaOS-2), showing that comparable lifetime ratio is measured independent of the magnesium concentration, while the amplitude ratio is significantly higher for control SaOS-2 cells than for deprived ones (Mann-Whitney test, $p < 0.0001$). This result indicates that the amplitudes of the DCHQ5 fluorescence components are related to the average Mg intracellular content. Further, by the amplitude ratio (A1/A2) it is possible to distinguish between cells having a difference of about 20 mM in their total intracellular Mg concentration, as the case of the sister cell lines employed in this study (Fig. 1D). However, the fluctuation of Mg concentration within a single cell is much smaller,[17] making more challenging the task of mapping local Mg intracellular compartmentalization. In fact, in all the single cells analyzed we did not find a statistical relevant difference in the amplitude ratio (A1/A2) between the AOIs corresponding to different steady state fluorescence intensities, although the data reported in Fig. 3 might suggest a trend in the expected direction.

We also performed analogous measurements on an additional cell line of human colon carcinoma (LoVo) known to have a lower intracellular Mg concentration with respect to SaOS-2 cells[17](Suppl. Inf Fig 1S and table 1S). The amplitude ratio of LoVo cells is lower than that of SaOS-2, which is consistent with the different intracellular Mg content. However, it should be pointed out that different cell lines, coming from different tissues have different biochemical and metabolic characteristics, making the comparison less significant than that obtained comparing same cell types.

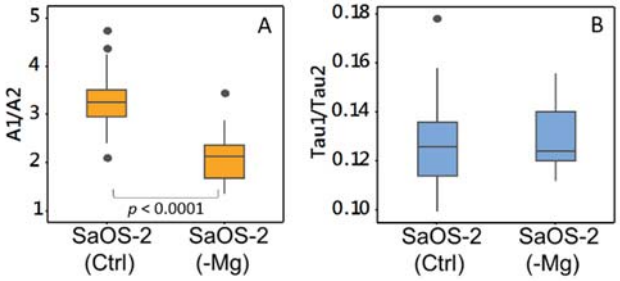

Fig. 4 Boxplot of the fluorescence amplitude ratio (A) and lifetime ratio (B) obtained from control (Ctrl) and Mg-deprived (-Mg) SaOS-2 cells.

Conclusions

In conclusion, we present the first detailed analysis of FLIM applications for Mg cell imaging. We employed the fluorescent dye DCHQ5, a derivative of diaza-18-crown-6 ethers appended with two 8-hydroxyquinoline groups, obtaining FLIM maps of magnesium in live cells and most important showing that the ratio of the amplitude terms of the bi-exponential equation of the fluorescence lifetime decay is related to the average magnesium intracellular concentration.

We provided the evidence that information on intracellular Magnesium concentration can be obtained performing

(steady state) confocal imaging of the proposed fluorescent probe under visible light excitation, as the time domain features of its fluorescence are not affected by its subcellular compartmentalization. In addition, using the same cell type with a difference in Mg content, we determined that the Mg intracellular concentration influences the amplitude of the lifetime decay relying on the fact that any changes in the FLIM data can only originate from changes in Mg intracellular concentration. It should be underlined that these conclusions could not be drawn by comparing different cell lines, which, although having different Mg concentration, also have very different intracellular environment, coming from different tissues and/or different animal species, eventually having different biochemical and physiological characteristics.

From a more general perspective, these results represent a proof-of-principle for the application of FLIM to element analysis in live cells. More in particular, they indicate that the analytical properties of DCHQ5 can be potentially exploited to perform Mg quantitative imaging analysis by conventional confocal microscopy.

Conflicts of interest

The authors declare no competing financial interests.

Acknowledgements

This work was supported by the RFO (Ricerca Fondamentale Orientata) of the University of Bologna and by the EU COST Action MP1401: "Advanced fibre laser and coherent source as tools for society, manufacturing and lifescience".

Notes and references

1 F. S. Wouters, P. J. Verveer and P. I. Bastiaens, *Trends Cell Biol.*, 2001, **11**, 203–211.
2 Q. S. Hanley, V. Subramaniam, D. J. Arndt-Jovin and T. M. Jovin, *Cytometry*, 2001, **43**, 248–260.
3 R. Cubeddu, D. Comelli, C. D'Andrea, P. Taroni and G. Valentini, *Journal of Physics. D, Applied Physics*, 2002, **35**, R61–R76.
4 P. J. Tadrous, J. Siegel, P. M. French, S. Shousha, E.-N. Lalani and G. W. Stamp, *J. Pathol.*, 2003, **199**, 309–317.
5 K. Itoh, K. Isobe and W. Watanabe, *Functional Imaging by Controlled Nonlinear Optical Phenomena*, John Wiley & Sons, 2013.
6 H. Szmacinski and J. R. Lakowicz, *J Fluoresc*, 1996, **6**, 83–95.
7 G. Farruggia, S. Iotti, L. Prodi, M. Montalti, N. Zaccheroni, P. B. Savage, V. Trapani, P. Sale and F. I. Wolf, *J. Am. Chem. Soc.*, 2006, **128**, 344–350.
8 H. M. Kim, C. Jung, B. R. Kim, S.-Y. Jung, J. H. Hong, Y.-G. Ko, K. J. Lee and B. R. Cho, *Angew. Chem. Int. Ed. Engl.*, 2007, **46**, 3460–3463.
9 C. Yu, Q. Fu and J. Zhang, *Sensors (Basel)*, 2014, **14**, 12560–12567.
10 G. Farruggia, S. Iotti, M. Lombardo, C. Marraccini, D. Petruzziello, L. Prodi, M. Sgarzi, C. Trombini and N. Zaccheroni, *Journal of Organic Chemistry*, 2010, **75**, 6275–6278.
11 C. Marraccini, G. Farruggia, M. Lombardo, L. Prodi, M. Sgarzi, V. Trapani, C. Trombini, F. I. Wolf, N. Zaccheroni and S. Iotti, *Chem. Sci.*, 2012, **3**, 727–734.
12 A. Sargenti, G. Farruggia, E. Malucelli, C. Cappadone, L. Merolle, C. Marraccini, G. Andreani, L. Prodi, N. Zaccheroni, M. Sgarzi, C. Trombini, M. Lombardo and S. Iotti, *Analyst*, 2014, **139**, 1201–1207.
13 A. Sargenti, G. Farruggia, N. Zaccheroni, C. Marraccini, M. Sgarzi, C. Cappadone, E. Malucelli, A. Procopio, L. Prodi, M. Lombardo and S. Iotti, *Nat Protoc*, 2017, **12**, 461–471.
14 J. McGinty, K. B. Tahir, R. Laine, C. B. Talbot, C. Dunsby, M. A. A. Neil, L. Quintana, J. Swoger, J. Sharpe and P. M. W. French, *J Biophotonics*, 2008, **1**, 390–394.
15 S. M. Kaiser and B. I. Escher, *Environ. Sci. Technol.*, 2006, **40**, 1784–1791.
16 G. Farruggia, S. Iotti, L. Prodi, N. Zaccheroni, M. Montalti, P. B. Savage, G. Andreani, V. Trapani and F. I. Wolf, *J Fluoresc*, 2008, **19**, 11–19.
17 E. Malucelli, A. Procopio, M. Fratini, A. Gianoncelli, A. Notargiacomo, L. Merolle, A. Sargenti, S. Castiglioni, C. Cappadone, G. Farruggia, M. Lombardo, S. Lagomarsino, J. A. Maier and S. Iotti, *Anal Bioanal Chem*, 2018, **410**, 337–348.